

# Predicting the decay time of solid body electric guitar tones

Arthur Paté,<sup>a)</sup> Jean-Loïc Le Carrou, and Benoît Fabre

*Sorbonne Universités, UPMC Univ Paris 06, UMR CNRS 7190, Institut Jean le Rond d'Alembert/LAM, 11, rue de Lourmel, F-75015, Paris, France*

(Received 19 December 2013; revised 28 March 2014; accepted 3 April 2014)

Although it can be transformed by various electronic devices, the sound of the solid body electric guitar originates from, and is strongly linked with, the string vibration. The coupling of the string with the guitar alters its vibration and can lead to decay time inhomogeneities. This paper implements and justifies a framework for the study of decay times of electric guitar tones. Two damping mechanisms are theoretically and experimentally identified: the string intrinsic damping and the damping due to mechanical coupling with the neck of the guitar. The electromagnetic pickup is shown to not provide any additional damping to the string. The pickup is also shown to be far more sensitive to the out-of-plane polarization of the string. Finally, an accurate prediction of the decay time of electric guitar tones is made possible, whose only requirements are the knowledge of the isolated string dampings and the out-of-plane conductance at the neck of the guitar. This prediction can be of great help for instrument makers and manufacturers.

© 2014 Acoustical Society of America. [<http://dx.doi.org/10.1121/1.4871360>]

PACS number(s): 43.75.Gh, 43.75.Yy, 43.40.At [JW]

Pages: 3045–3055

## I. INTRODUCTION

The solid body electric guitar is an electric guitar without soundbox in order to avoid acoustic feedback that occurs when an amplifier is used. The soundbox is replaced by a thick and solid wood plate. The low admittance at the bridge provides at the same time much more sustain than hollow body electric guitars, which have a thin soundboard. The instrument is equipped with electromagnetic pickups, transducing mechanical string vibration into an electric signal.<sup>1,2</sup> This signal is sent to an amplifier and the sound is radiated by loudspeakers. In addition to the chance that has been given to the guitar player to get heard among other instruments, the electrification of the guitar has thoroughly changed the playing techniques and musical philosophy of guitar players.

There has been a constantly increasing number of devices transforming the signal of the pickup before getting into the amplifier, so that the effect processing chain itself has become a real instrument. Acoustical studies about the electric guitar have been, so far, mainly focused on this effect chain, from pickup<sup>3,5,6</sup> to amplifier<sup>7,8</sup> through effect processing devices,<sup>9,10</sup> often aiming at doing sound synthesis,<sup>11</sup> post-processing on the output signal of the pickup,<sup>12</sup> or analysis of music and technology.<sup>13,14</sup>

The pickup and the electric chain are, of course, essential for the sound of the electric guitar, but the pre-transduction mechanical phenomena also contribute to the sound. The string is coupled at both its ends to other vibrating systems. Mechanical coupling with these systems (fret,<sup>15–17</sup> bridge, finger, fingerboard, nut) alters the string vibration. Gough<sup>18</sup> studied the coupling between a string and a resonant structure in the general case of a string instrument: If the frequencies of the separated systems are close, the frequencies and dampings

of the coupled system might be altered. This result was confirmed in the case of duplex piano strings coupled by the bridge<sup>19</sup> and in the case of the coupling of a classical guitar string with the soundboard.<sup>20</sup> Similar results are found for the harpsichord case,<sup>21</sup> where the coupling of the string and the soundboard changes the decay time of the string.

Despite its name, the solid body electric guitar vibrates.<sup>22–25</sup> Only a few studies investigated the mechanics of the instrument in connection with its musical features. Fleischer<sup>26,27</sup> studied the “dead spot” phenomenon: some notes have a much shorter decay time than their neighbors. This phenomenon has been qualitatively linked with the dynamic behavior of the guitar. At the frequency of the note, the guitar may have a high out-of-plane conductance value at the place where the note is played. The string vibrating energy may be caught by the structure. The length of the note, the sustain, is affected by the coupling. Partials may couple differently so timbre inhomogeneities may appear. For the solid body electric bass guitar, the global decay time is shown<sup>28</sup> to move away from the theoretical isolated string decay time if there are some out-of-plane conductance peaks at string partial frequencies.

The present paper gives the experimental and theoretical justifications for the implementation of a framework for the study of solid body electric guitar tones' decay. The aim of the article is to identify which damping mechanisms are relevant for the prediction of decay time, among those suggested by various sources: intrinsic string damping, coupling with the structure, magnetic interaction with the pickup.

Section II simplifies the complex mechanical system of the solid body electric guitar to a string connected to a mobility at one of its ends. The isolated string behavior is theoretically and experimentally investigated in Sec. III. The coupling of the string with the magnetic field and the structure is the object of Sec. IV. Finally, Sec. V proposes an estimation method of the global decay time only based on the knowledge of the mechanical behavior of the structure and the  $Q$  values of the isolated string.

<sup>a)</sup>Author to whom correspondence should be addressed. Electronic mail: [pate@lam.jussieu.fr](mailto:pate@lam.jussieu.fr)

## II. AN ELECTRIC GUITAR MODEL

### A. The guitar of the study

A handmade replica of the reference model<sup>1</sup> *Les Paul Junior* by *Gibson* illustrates the study. According to the specifications of the historical model, body and neck are made of mahogany, the fingerboard is made of rosewood, and one single-coil *P-90* pickup made by manufacturer *Kent Armstrong* is mounted near the bridge. This is a copy of one of the most popular and widespread electric guitar pickups, originally made by manufacturer *Gibson*.<sup>29</sup>

The string of the electric guitar is stretched between the bridge and the peg. The vibrating length of an open string is from the bridge to the nut. The basic role of the left hand (of a right-handed player) is to shorten this vibrating length in order to produce other playing frequencies. By doing this, the left-hand finger pushes the string against the fret. Figure 1 gives an overview of the mechanical interaction processes between the string and the other parts of the guitar in a playing context. It defines the axes that will be used in the following of the article:  $x$  is the axis of the string,  $y$  is parallel to the fret (the “in-plane” direction), and  $z$  is normal to the guitar body’s plane (“out-of-plane”). The interactions between the strings and the other parts of the guitar alter the vibration of the string.

### B. String model

The knowledge of the bandwidth of the pickup allows us to make some simplifications of the string model. All notes of the guitar in the study are played successively by an experienced player. Plucking is performed with a pick and fingering with the left-hand middle finger. The plucking point is at a typical distance of 12 cm from the bridge. Care has been taken to keep the plucking (essentially along the  $y$  axis in Fig. 1) as reproducible as possible, which is the case for an experienced player’s gesture.<sup>30</sup> The pole pieces of the pickup are at a distance of 4 cm from the bridge. The output of the pickup is recorded. From the spectrum  $X$  of the whole recording (all notes played in a row, without any normalization), the cumulative energy contained between 0 Hz and each frequency is computed as

$$E(f) = \int_0^f |X(\nu)|^2 d\nu. \quad (1)$$

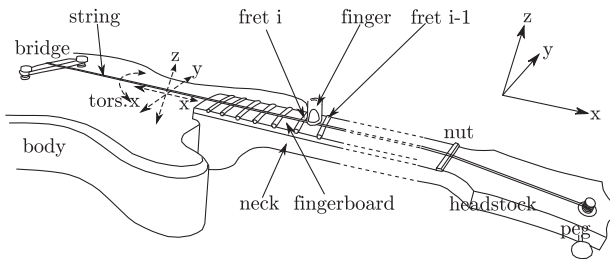


FIG. 1. Overview of the mechanical interactions between the string and the structure of an electric guitar. The string is stretched between the bridge and the peg. Energy flows from the string to the structure at several places: Bridge, fret, finger, nut, peg. Transverse string vibration along  $y$  and  $z$  axes, as well as longitudinal waves along  $x$  axis and torsional waves around  $x$ -axis can occur (dashed lines with arrows).

As can be seen in Fig. 2, 95% of the energy of the output signal of the guitar is below the cutoff frequency of 2.5 kHz. This confirms Karjalainen’s<sup>12</sup> results about the low-pass behavior of electric guitar pickups.

A string of length  $L$ , Young’s modulus  $E$ , shear modulus  $G$ , diameter  $d$ , moment of area  $I$ , mass per unit length  $\rho_L$ , and density  $\rho_V$  is considered. This paper focuses on the 3rd (note G3) string, but all results can be extended to the other strings. Geometric characteristics measured on a G string from the *d’Addario EXL110* set as well as theoretical material data are shown in Table I. Calculated data from measured and theoretical data are shown in Table II.

The unperturbed case is a string stretched between two rigid ends with tension  $T$ . Torsional waves around the  $x$  axis can travel with celerity  $c_{\text{tors}} = \sqrt{G/\rho_V}$  and longitudinal waves along the  $x$  axis can travel with celerity  $c_{\text{comp}} = \sqrt{E/\rho_V}$ , so that the lowest frequency for each of these wave types is the fundamental frequency defined as<sup>31</sup>

$$f_0^{\text{tors, comp}} = \frac{1}{2L} c_{\text{tors, comp}}. \quad (2)$$

Table II shows that the values of  $f_0^{\text{tors}}$  and  $f_0^{\text{comp}}$  are above the cutoff frequency of the pickup, so longitudinal and torsional waves would not significantly contribute to the sound of the guitar. Furthermore, the pickup is sensitive to the change in the magnetic flux through its coil.<sup>4</sup> Unless the string is strongly inhomogeneous, such change should be very small for longitudinal or torsional waves.

Considering bending waves, the motion  $\hat{z}$  of the string along axis  $z$  in a frictionless approach is governed by<sup>31</sup>

$$\frac{1}{c^2} \frac{\partial^2 \hat{z}}{\partial t^2} = \frac{\partial^2 \hat{z}}{\partial x^2} - \frac{EI}{T} \frac{\partial^4 \hat{z}}{\partial x^4}, \quad (3)$$

where  $c = \sqrt{T/\rho_L}$  is the velocity of transverse waves. Note that everywhere in the following equations of string, the polarization  $\hat{z}$  can be replaced by the polarization  $\hat{y}$  of the string. Considering harmonic waves, the Eq. (3) leads to

$$\omega_{0,n} = k_{0,n} c \sqrt{1 + k_{0,n}^2 \frac{EI}{T}}, \quad (4)$$

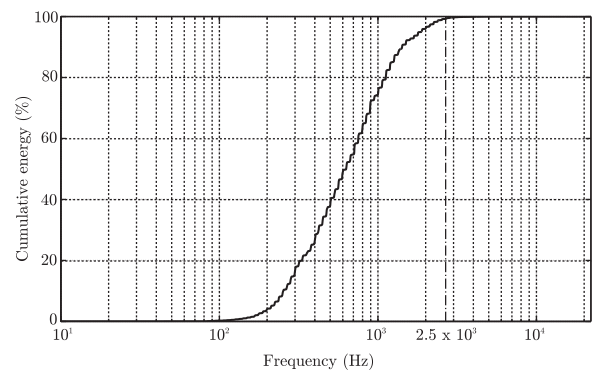


FIG. 2. Cumulative energy between 0 Hz and the current frequency, computed on a recording of all the notes of the guitar played in a row. Dashed-dotted line indicates the frequency 2.5 kHz, above which less than 5% of the total energy remains.

TABLE I. Measured and theoretical data for the G3 string. Measured data:  $d$ , diameter;  $L$ , open string length;  $\rho_L$ , mass per unit length. Computed data:  $I = \pi d^4/64$ , second moment of area;  $c = \sqrt{T/\rho_L}$ , velocity of transverse waves;  $T$ , tension. Theoretical data:  $E$ , Young's modulus of steel;  $G$ , shear modulus of steel.

$d$ (m)	$I$ (m <sup>4</sup> )	$L$ (m)	$\rho_L$ (kg m <sup>-1</sup> )
$4.32 \times 10^{-4}$	$1.71 \times 10^{-15}$	0.629	$1.1 \times 10^{-3}$
$c$ (m s <sup>-1</sup> )	$T$ (N)	$E$ (Pa)	$G$ (Pa)
246.43	69.43	$2 \times 10^{11}$	$8.08 \times 10^{10}$

where the index 0 reminds that the quantities correspond to an isolated string, and  $n$  denotes the partial number. Equation (4) can be written with the inharmonicity<sup>32</sup> coefficient  $\beta = EI\pi^2/TL^2$ :

$$\omega_{0,n} = k_{0,n}c\sqrt{1 + n^2\beta}. \quad (5)$$

For the 3rd string, the highest inharmonicity coefficient is reached for the shortest vibrating length (string pressed against 22nd fret)  $L = 0.117$  m and equals  $\beta_{\max} = 1.16 \times 10^{-3}$  according to Table I. The corresponding note is a F5 with fundamental frequency 698.46 Hz. Within the frequency range of the study (upper limit 2.5 kHz, see Fig. 2), this note has three overtones, leading to a maximum value of  $n^2\beta_{\max} = 3^2\beta_{\max} = 0.0104$ . The frequency ratio between the flexible string frequency and the stiff string frequency is then  $1/\sqrt{1 + 3^2\beta_{\max}} = 0.9948$ . Between a flexible and a stiff string model, a frequency change of 0.52% occurs in the worst case for the considered string.

Assuming then a flexible string model, Eq. (4) becomes

$$\omega_{0,n} = k_{0,n}c. \quad (6)$$

Rigid-end boundary conditions  $\hat{z}(0, t) = 0$  and  $\hat{z}(L, t) = 0$  drive to the classic form of string motion:

$$\hat{z}(x, t) = \sum_{n=1}^N a_{0,n} \cos(2\pi f_{0,n}t + \phi_{0,n}) \sin(k_{0,n}x), \quad (7)$$

where  $a_{0,n}$  are the modal amplitudes,  $f_{0,n}$  are the modal frequencies,  $\phi_{0,n}$  are the phases,  $k_{0,n} = n\pi/L$ ,  $n = 1, 2, \dots$  are the quantized wavenumbers, and  $N$  is the number of harmonics within the bandwidth of interest.

Since the string is considered here as flexible, it is assumed that no bending moment is transmitted to the string part between the fret denoted as “fret  $i$ ” in Fig. 1 and the peg. This fret  $i$  can be considered a string end. The mechanical interactions between the string and the finger, the fret  $i-1$ , the nut, and the peg can be neglected.

TABLE II. Data computed from the G3 string characteristics.  $f_0$ ,  $f_0^{\text{tors}}$ , and  $f_0^{\text{comp}}$  are the fundamental frequencies for respectively transverse, torsional, and longitudinal vibration.

$f_0$ (Hz)	$f_0^{\text{tors}}$ (Hz)	$f_0^{\text{comp}}$ (Hz)
196	2558	4125

Following Fleischer,<sup>26,27</sup> the conductance is found in Sec. IV B to be much smaller at the bridge than at the fret. The bridge end of the string is then considered as rigid in the following.

The interactions between the string and the structure can be modeled by the two transverse polarizations of a flexible string connected at one end to a mechanical 2D-mobility  $Y$ . This mechanical model is shown in Fig. 3.

### III. THE ISOLATED STRING

In order to estimate the intrinsic losses of the string, the string is first studied separately from the guitar.

#### A. A model of string damping

A complete review of the damping mechanisms of an isolated string is presented by Valette.<sup>31</sup> The damping in musical strings being small, it can be inserted by adding an imaginary part to the string modal frequencies:<sup>33</sup>

$$f_{0,n} \rightarrow f_{0,n} \left( 1 + \frac{j}{2Q_{0,n}} \right), \quad (8)$$

where  $j$  is the imaginary unit and  $Q_{0,n}$  is the modal  $Q$  factor (or quality factor) associated with the  $n$ th partial. According to Valette,<sup>31</sup>  $Q_{0,n}$  is due to several mechanisms. A part of the  $Q$  factor is due to the friction of the string with the air:

$$Q_{\text{friction},n}^{-1} = \frac{R_L}{2\pi\rho_L f_n} \frac{1}{f_n}, \quad (9)$$

where

$$R_L = 2\pi\eta_{\text{air}} + 2\pi d\sqrt{\pi\eta_{\text{air}}\rho_{\text{air}}f_n}, \quad (10)$$

where  $\eta_{\text{air}}$  and  $\rho_{\text{air}}$  are the air dynamic viscosity and density, respectively.

Internal damping mechanisms also contribute to the total  $Q$  factor. We denote VE and TE the effects of visco and thermo-elastic phenomena, respectively:

$$Q_{\text{VE/TE},n}^{-1} = \frac{4\pi^2 EI}{T^2 c} (\delta_{\text{VE}} + \delta_{\text{TE}}) f_n^2, \quad (11)$$

where  $\delta_{\text{VE}}$  and  $\delta_{\text{TE}}$  are the imaginary parts of the Young's modulus.

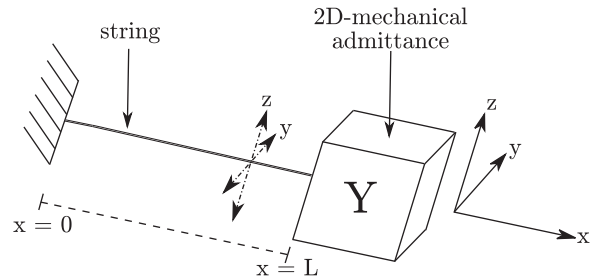


FIG. 3. Scheme of the fully simplified coupled system standing for the solid body electric guitar: a string moving in two orthogonal polarizations connected to a 2D-mobility  $Y$ .

Another damping mechanism occurs in wound strings, associated with dry friction between two successive turns of wire. It comes out as a delay between the slope  $\partial \hat{z} / \partial x$  and the shear force  $T(\partial \hat{z} / \partial x)$  in the string, hence the effect is the same as that of a complex tension  $T(1 + j\delta_W)$ .

The last damping mechanism is due to the dislocation phenomenon. It was shown<sup>34</sup> to be well described by a factor  $Q_{\text{disl}}$ , which is constant over the audio frequency range.

Finally, the damping of the  $n$ th string partial of the isolated string is

$$Q_{0,n}^{-1} = Q_{\text{VE/TE},n}^{-1} + Q_{\text{friction},n}^{-1} + Q_{\text{disl}}^{-1}. \quad (12)$$

For a wound string, the term  $Q_W^{-1} = \delta_W$  should be added to Eq. (12). Experimental values of the  $Q$  factor are estimated in Sec. III D with the method described in Sec. III C.

## B. Experimental protocol

A heavy, rigid, and damped measurement frame<sup>35,36</sup> is used to guarantee rigid-end conditions to the string, so that the string is considered to be isolated. Two optical sensors<sup>37</sup> are used to record each transverse polarization of the string vibration: As the string vibrates between the optical emitter and receiver, it periodically and gradually cuts off the optical beam. Before each measurement, string rest position and optical beam are carefully set up in such a way that the whole motion of the string remains in the linear part of the characteristic function of the optical sensor.

The G3 string is first set and tuned to its nominal open string length and fundamental frequency according to Table I. The length of the string is then shortened step by step to the vibrating lengths corresponding to all the bridge-fret distances. Tension, vibrating lengths, and playing frequencies are the same as if the string was mounted on a guitar.

For each string length, the optical sensors and the end of the string are at a distance of 4 cm, because it is the distance between the bridge and the pickup's pole pieces on the guitar of the study. For each length, the string is excited 8 times with the wire-breaking<sup>20</sup> method. The excitation angle between axes  $y$  and  $z$  is  $45^\circ$  in order to excite both polarizations identically. The end of the string and the excitation point are at a typical playing distance of 12 cm. Figure 4 shows the experimental setup for the study of the isolated string.

## C. Signal model

The modal  $Q$  factors of Eq. (8) can be inserted in the complex form of Eq. (7). The string vibration measurements are made at a particular place  $x = x_{\text{meas}}$ , so that the spatial term  $\sin(k_{0,n}x_{\text{meas}})$  of Eq. (7) is a constant and can be included in the modal amplitudes. The signal model then writes

$$x(t) = \sum_{n=1}^N a_n \cos(2\pi f_n t + \phi_n) e^{(-\pi f_n / Q_n) t}. \quad (13)$$

Note that the index 0 is omitted because this model is applied for the isolated as well as the coupled string. This signal model is known as exponential sinusoid model (ESM). A natural choice of analysis method for such signals is the ESPRIT

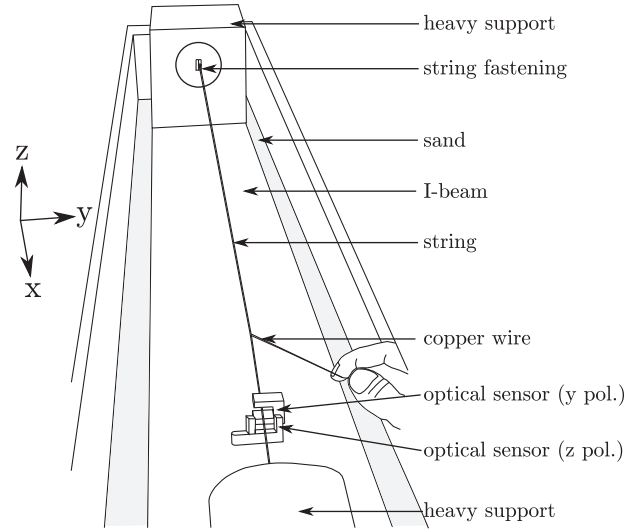


FIG. 4. Sketch of the measurement setup for the isolated string. The string is stretched between two heavy supports at playing tension and length. Two optical sensors measure each transverse ( $y$  and  $z$ ) polarization. The string is excited with the wire-breaking method. Clamps firmly attach the string's heavy supports as well as the optical sensors' supports to a heavy I-beam filled with sand, and are not drawn here for clarity reason.

method.<sup>38</sup> This method accurately<sup>39</sup> identifies the modal amplitudes  $a_n$ , frequencies  $f_n$ , phases  $\phi_n$ , and  $Q$  factors  $Q_n$ .<sup>39,40</sup> Furthermore the ESPRIT method overcomes the Fourier resolution, making possible the study of coupled systems with very close frequencies.<sup>39</sup> This is an expected feature of the string signals when dealing with the two polarizations.

The method proposed by Le Carrou<sup>39</sup> is applied here to the string signals, for the purpose of accuracy. The analysis is carried out where the exponential decay assumption is valid: Because the focus of this paper is the notes' decay, the attack part of the tones are not considered, although it contributes a lot to the tone quality of electric guitars. In order for the ESPRIT algorithm not to be disturbed by the transient components, the portion of the signal that is analyzed starts 2–3 s after the onset time. A duration of 1–2 s for the analyzed signal portion is enough to get accurate results and to avoid a lower signal-to-noise ratio at the end of the vibration. The corresponding spectrum is shifted so that it is centered around the frequency of interest. A very high  $Q$  factor low-pass filter is then applied to the signal, in order to let the algorithm focus on this very frequency. A high decimation factor allows then a strong reduction of the computational time without loss of information. The ESPRIT method is applied to the resulting signal. The implementation of the ESPRIT method itself is explained in a very comprehensive way in recent papers<sup>39,40</sup> dealing with closely related topics.

## D. Results

The ESPRIT method is applied to the output signals of the optical sensors. This section gives the results for the isolated string, at vibrating lengths corresponding to the vibrating lengths defined by the successive frets when the string is mounted on the guitar. The measurement frame is known<sup>34</sup> to be symmetric. This is confirmed by the fact that the results are similar for both polarizations. Only one polarization is



therefore shown. For each vibrating length,  $Q$  values are identified by the method described above for every partial under 1000 Hz, since the vibratory study of Sec. IV is limited to this frequency. For all vibrating lengths and partials within the bandwidth, the identified  $Q$  factors are shown in Fig. 5. The mean values as well as the expanded uncertainty of eight measurements are shown. Expanded uncertainties (due to measurement and the ESPRIT identification method) for the identification of  $Q$  factors are found to be small. This proves the repeatability of the measurement protocol. The data of Fig. 5 is compared to the computation of the isolated string damping model of Eq. (12). For the computation, the values of Table I, as well as typical values,<sup>31</sup> are used:  $\delta_{\text{VE/TE}} = 1 \times 10^{-3}$ ,  $\rho_{\text{air}} = 1.2 \text{ kg m}^{-3}$  and  $\eta_{\text{air}} = 1.8 \times 10^{-5} \text{ kg m}^{-1} \text{ s}^{-1}$ . The  $Q$  factor due to dislocation is adjusted to  $Q_{\text{disl}} = 5500$ . Note that small differences between the model prediction and the measurements can be observed. Indeed, the experimental estimation of  $\delta_{\text{VE,TE}}$  and  $Q_{\text{disl}}$  is still a challenging problem. Depending on the composition of the metal used for the musical string,  $\delta_{\text{VE,TE}}$  takes values ranging from  $1 \times 10^{-4}$  to  $1 \times 10^{-3}$ . The variation range of  $\delta_{\text{VE,TE}}$  as well as the uncertainty in its measurement are quite high. However, since in the frequency band of the study, the isolated string damping is dominated by air friction, the uncertainty in  $\delta_{\text{VE,TE}}$  should not have a significant effect. The reasonably assumed frequency-independent  $Q_{\text{disl}}$  strongly depends on the history of the metal (cold working for example) and can take values from 7000 to 80 000 for brass strings.<sup>34</sup> In absence of devoted study about  $Q_{\text{disl}}$ , this parameter is estimated by fitting the theoretical  $Q$ -curve to experimental  $Q$ -values.

A gray line in Fig. 5 shows the isolated string damping model computation. As can be seen, for all vibrating lengths and partials in the frequency range, the values of the model are always included within the experimental uncertainties, so the data and the model match. A small but systematic trend can be noticed in Fig. 5: lower (respectively, upper) components seem to have a slightly lower (respectively, higher)  $Q$  factor than predicted by the model.

However, the damping model of Eq. (12) that was developed for harpsichord strings is still valid for the

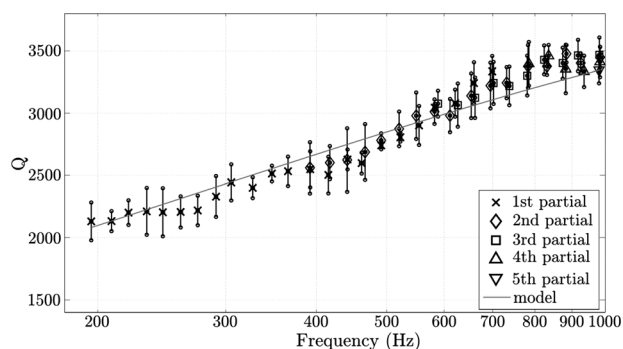


FIG. 5. Isolated G3 string: Identified  $Q$  factors for every vibrating length (corresponding to every bridge-to-fret distance) and every partial below 1000 Hz. For each vibrating length, eight measurements are carried out. For both frequency and  $Q$  factor, crosses (respectively, diamond, square, upward triangle, and downward triangle) indicate the mean value, and circles indicate the expanded uncertainty (95% confidence interval) for the 1st (respectively, 2nd, 3rd, 4th, and 5th partial). Gray line indicate the results of the isolated lossy string model of Eq. (12).

considered electric guitar string. Note that for electric bass guitar strings, the main damping mechanism seems to be the internal friction<sup>28</sup> (denoted  $Q_{\text{VE/TE}}$  here) whereas here the electric guitar string damping is dominated by  $Q_{\text{friction}}$ , the term representing the friction of the string with the air. The isolated string behavior has been described, now its coupling with the guitar will be studied.

## IV. THE STRING AND THE GUITAR

When it is mounted on the guitar, the string can couple with the magnetic pickup and the mechanical structure. The two couplings are investigated in this section.

### A. On the influence of the pickup

The influence of the pickup on the string vibration is subject to debate among the luthiers community. An attracting force may result from a magnetic interaction between the pickup pole pieces and the ferromagnetic string. This may induce an extra damping for the string. The influence of the pickup on the string vibration is studied experimentally.

The *Kent Armstrong P-90* pickup of the guitar presented in Sec. I is used in this study. Both the pickup and the G3 string are separated from the guitar. Excitation and displacement measurement methods remain the same as in Sec. III B. The pickup is also at a distance of 4 cm from the string end. Fifteen measurements are carried out in each of the following cases: isolated string alone and four cases with the pickup in the vicinity of the mechanically isolated string. Two typical distances between the string at rest position and the corresponding pole piece of the pickup are investigated: 3 and 4 mm. These distances correspond to two normal settings for an electric guitar. For each of these distances, the pickup can be either plugged to an actuated guitar amplifier or not plugged at all (open-circuit). The  $Q$  factors of the fundamental frequency are identified with the ESPRIT method and plotted in Fig. 6. The recorded string polarizations are parallel and perpendicular to the pickup pole piece. For both polarizations of the transverse vibration and for all configurations of string and pickup, the  $Q$  factors take similar values, and stay in the same uncertainty range. The extra string damping due to a magnetic interaction with the present pickup is found to be negligible. The following of the article will therefore only consider the coupling of the string with the structure.

### B. Coupling the string with the structure

The interactions between the string and the structure can be described as shown in Fig. 3. Let the string end at  $x = 0$  be attached to the bridge and that at  $x = L$  be connected to the 2D-mobility  $Y$  representing the neck.  $Y$  can be written as

$$Y = \begin{pmatrix} Y_{YY} & Y_{YZ} \\ Y_{ZY} & Y_{ZZ} \end{pmatrix}, \quad (14)$$

where  $Y_{ij}$  is the  $ij$ -mobility defined as the ratio in the frequency domain between the velocity along the  $i$  axis and the exciting force applied along the  $j$  axis. According to the reciprocity principle, the non-diagonal terms  $Y_{ZY}$  and

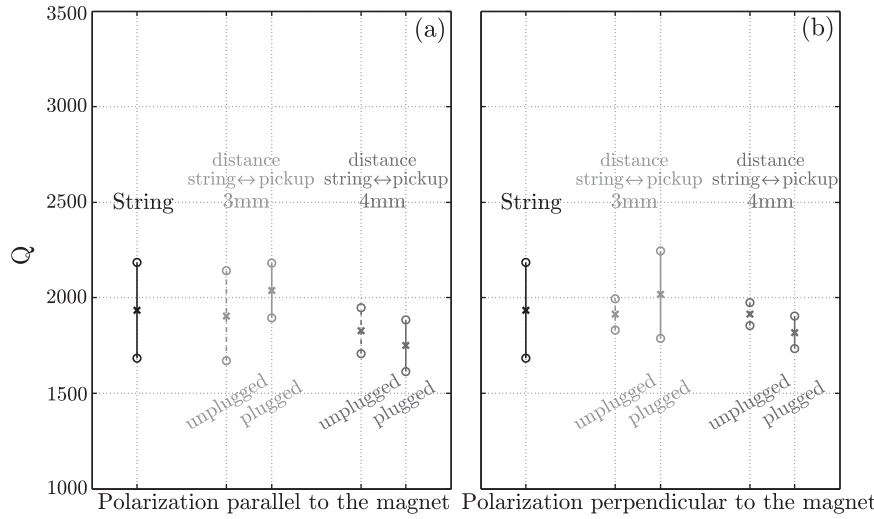


FIG. 6. Identified  $Q$  factors for the fundamental frequency of the unmounted string, with or without pickup at its vicinity. Two typical distances between the string and the magnetic pole piece are studied. Pickup can be either in open-circuit or plugged into the amplifier. Crosses indicate the mean value and circles indicate the expanded uncertainty (95% confidence interval) of 15 measurements. (a) Polarization parallel to the pole piece ( $z$ ), (b) polarization normal to the pole piece ( $y$ ).

$Y_{YZ}$  are assumed to be equal. Note that the terms involving the  $x$  axis are neglected since they interact with the longitudinal waves in the string, which are neglected (see Sec. II B).

A classical frequency response measurement method is used to identify all terms of the matrix  $Y$ . They are measured at each fret along G3 string's axis. The specific shape of the "wrap-around" bridge does not allow to measure in-plane conductance with an accuracy as great as the out-of-plane conductance. However,  $Y_{YY}$  and  $Y_{ZY}$  measurements at the bridge are shown in Fig. 7 for comparison. The impulse force is applied by a *PCB Piezotronics 086C01* impact hammer while a *PCB Piezotronics 352C65* accelerometer provides the acceleration signal. The mass of the accelerometer is  $2 \times 10^{-3}$  kg, which is small compared to the total mass 3.4 kg of the guitar. The hammer force limits the bandwidth of the whole study to 1000 Hz. Care is taken to have the force application point and the measurement point as close as possible, guaranteeing a true driving-point measurement. Only the conductance (real part of the mobility) measurements are shown in Fig. 7. These measurements are carried out on the axis of symmetry of the guitar, where no contribution of the torsional modes is expected. The mechanical coupling phenomenon is just the same for the other strings,

excepted that the presence of torsional modes increases the chance of coupling.

Figure 7 shows that the conductance at the bridge takes values up to  $1.76 \times 10^{-3} \text{ m s}^{-1} \text{ N}^{-1}$ . These values are small in comparison with the conductance values at the neck that can reach  $1.02 \times 10^{-1} \text{ m s}^{-1} \text{ N}^{-1}$  (which is in the same order of magnitude than the bridge admittance of classical guitars<sup>26</sup>). This high bridge impedance validates the assumption of a string connected at one end only (Sec. IV B). Figure 7 also shows that the cross-mobilities  $Y_{ZY}$  and  $Y_{YZ}$  are small as well, so will be neglected. Accordingly, only the coupling with  $ZZ$  and  $YY$  conductances will be investigated. For purposes of physical interpretation, Fig. 7 gives the results of a modal analysis associating each out-of-plane conductance peak with a modal shape.

From the string's point of view, the only change to the model of Sec. III is the end condition at  $x = L$ . Calculations are detailed for a transverse polarization coupled to a generic mobility  $\hat{Y}$  ( $\hat{Y} = Y_{YY}$  or  $\hat{Y} = Y_{ZZ}$ ).

The presence of a moving end can be satisfactorily described as small perturbation to the unperturbed wavenumbers:<sup>31</sup>

$$k_{0,n} \rightarrow k_n = \frac{n\pi}{L} + \delta_n, \quad (15)$$

where  $\delta_n \ll 1$ . For reasons of continuity, the string admittance must be equal to the structure mobility at the coupling point  $x = L$ :

$$\hat{Y}(L, \omega_{0,n}) = j \frac{\tan[(\frac{n\pi}{L} + \delta_n)L]}{Z_c}, \quad (16)$$

where  $Z_c = \sqrt{\rho_L T}$  is the characteristic impedance of the string.

Assuming that  $Z_c \hat{Y}(L, \omega_n) \ll 1$  to ensure the reflection of traveling waves at the end of the string, Eq. (16) leads to the expression of  $k_n$ :

$$k_n = \frac{n\pi}{L} - j \frac{\hat{Y}(L, \omega_{0,n})Z_c}{L}, \quad (17)$$

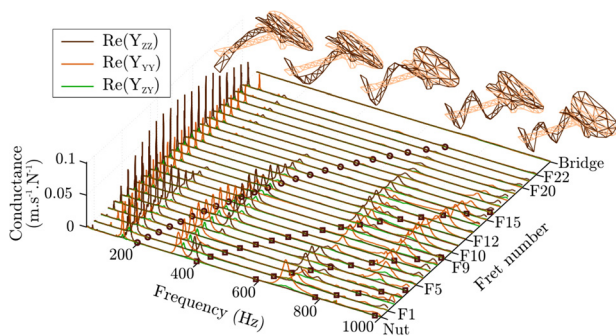


FIG. 7. (Color online) Out-of-plane ( $ZZ$ ), in-plane ( $YY$ ), and cross ( $ZY$ ) conductance along the G3 string's axis: at every fret and at the bridge. For each fret, circle and squares denote the string's fundamental frequency and partials respectively, for the considered bandwidth. A modal analysis allows us to identify the modes for each out-of-plane conductance peak, above which the corresponding mode shapes are drawn.

with which Eq. (6), with isolated string damping of Eq. (8), becomes

$$\omega_n = \frac{n\pi c}{L} \left[ 1 + \frac{j}{2Q_{0,n}} - j \frac{\hat{Y}(L, \omega_{0,n}) Z_c}{n\pi} \right]. \quad (18)$$

The perturbed modal frequencies are the real parts of the  $\omega_n$ , divided by a factor  $2\pi$ :

$$f_n = \frac{nc}{2L} \left[ 1 + \frac{n^2 \pi^2 EI}{L^2 2T} + \frac{Z_c}{n\pi} \text{Im}[\hat{Y}(L, \omega_{0,n})] \right], \quad (19)$$

while the perturbed  $Q$  factors are linked to the imaginary part of the  $\omega_n$ :

$$Q_n^{-1} = Q_{0,n}^{-1} + \frac{c^2 \rho_L}{\pi L} \text{Re}[\hat{Y}(L, \omega_n)] \frac{1}{f_n}. \quad (20)$$

Depending on the polarization of interest,  $f_n$  and  $Q_n$  values for  $z$  and  $y$  polarization are obtained by replacing  $\hat{Y}$  by  $Y_{ZZ}$  or  $Y_{YY}$ , respectively. It is checked that the imaginary part of the mobility is small enough to induce a very minor change in the modal frequencies. The two polarizations of the string mounted on the guitar will then have very slightly differing frequencies. Depending on the conductance, the two polarizations may significantly differ in terms of modal damping.

An illustration of the coupling described by Eq. (20) is given with two examples. Two coincidences between string and structure modes can be seen in Fig. 7 and magnified in Fig. 8:  $\text{Re}(Y_{YY})$  conductance takes a high value at 9th fret for the fundamental frequency of the note which is played at this place. The same happens to  $\text{Re}(Y_{ZZ})$  at 12th fret for the fundamental frequency of the corresponding note.

In order to experimentally measure the mounted-string  $Q$  factors for these two examples, the string is stretched at playing tension between the bridge and the nut of the guitar. Excitation and displacement measurement remain the same as in Sec. III B. Measurements with a capo at 9th and 12th frets are carried out. For both polarizations, the  $Q$  factors for the fundamental frequency of the mounted string signals are identified. In Fig. 9 they are compared to the corresponding measured  $Q$  factors of the isolated string. The  $Q$  values

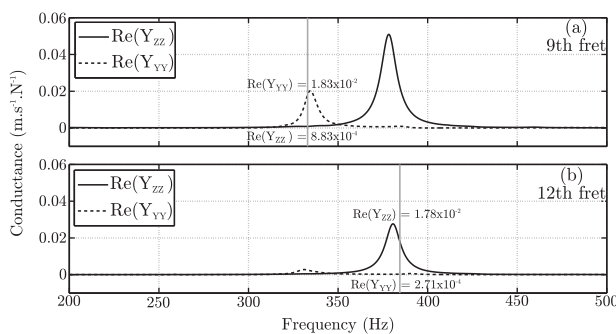


FIG. 8. Measured conductance at 9th fret (a) and 12th fret (b) along G3 string's axis. Solid line indicates out-of-plane conductance. Dashed line indicates in-plane conductance. The transverse gray line shows the fundamental frequency of the note produced on the G3 string at the corresponding fret. For this frequency, conductance values are given in  $\text{m s}^{-1} \text{N}^{-1}$ .

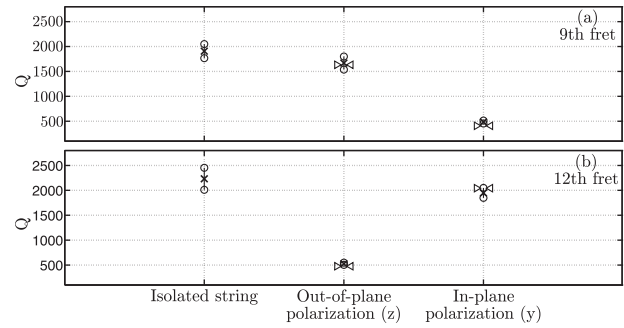


FIG. 9. Identified  $Q$  factor for the fundamental frequency of the note played at 9th fret (a) and 12th fret (b) of the G3 string. Both polarizations' results for the mounted string are compared to the isolated string. Circles and crosses indicate mean values and expanded uncertainty (95% confidence interval) respectively of 15 measurements. The arrows point out the  $Q$  value computed by the model of Eq. (20) with the isolated-string  $Q$  factors and the conductance values.

computed from the model of Eq. (20) with the string characteristics of Table I, the measured string-alone  $Q$  values and neck conductances are also presented in Fig. 9. As Fig. 9 shows, a good agreement between the experimentally measured  $Q$  factors and the model-computed  $Q$  factors is found. The coupling model is found to give a good quantitative prediction of the  $Q$  factors for every note. Note that the influence of the structure has only been evaluated in free conditions (the guitar lying on straps supported by a frame). In playing conditions, it is expected that the left hand as well as the right arm and the stomach provide some additional damping to the guitar modes. Such damping may lower the conductance value at the resonance frequency. As a consequence, at this very frequency string/structure coupling effects might be slightly different and the dead spots could be less disturbing in playing conditions.

### C. The pickup and the string polarizations

The previous section dealt with the coupling of both polarizations of the transverse string vibration. This section investigates the behavior of the pickup toward these two polarizations.

#### 1. Pickup's sensitivity to both polarizations

Jungmann<sup>5</sup> indicates that the output signal of the magnetic pickup of the electric guitar is mainly made up of the out-of-plane polarization. Horton and Moore<sup>4</sup> included this phenomenon in a pickup model. In order to have an experimental evidence of this phenomenon for the pickup of this study, a comparison of the pickup and optical sensors' signals is carried out. As in Sec. IV A, the string and the pickup are separated from the guitar. This time, the wire-breaking method is used for the excitation along each transverse axis successively. For each excitation, vibrations in each polarization as well as the output of the pickup are recorded. Since the magnetic pickup is sensitive to the velocity of the string,<sup>4</sup> the velocity of each polarization is computed from the optical displacement measurements. Typical results from a series of twenty measurements are shown in Fig. 10. The polarization perpendicular to the excitation has at least a 10 times smaller

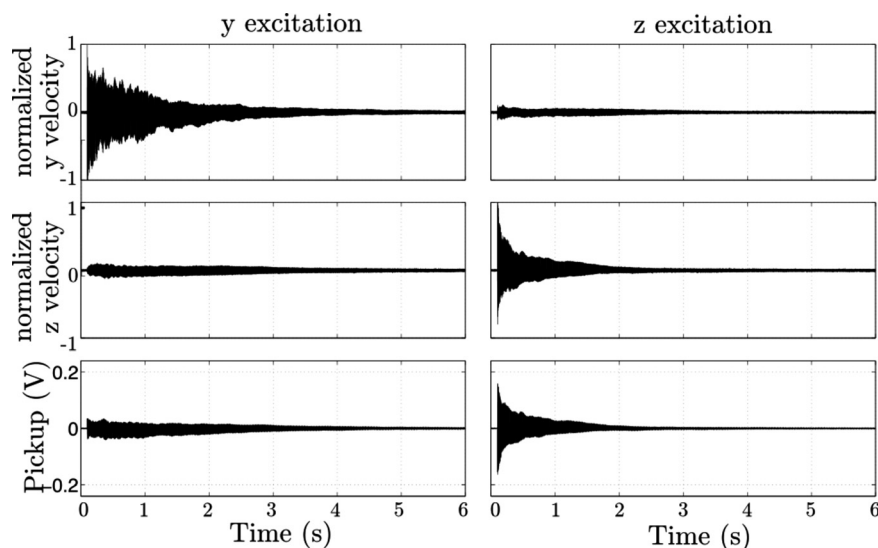


FIG. 10. String excited by the wire-breaking method, isolated from the guitar, at the vicinity of a pickup. The pickup is set so that the pole pieces are parallel to the  $z$  axis. For in-plane ( $y$ , left column) and out-of-plane ( $z$ , right column) excitation, corresponding waveshapes of in-plane ( $y$ , upper row) and out-of-plane ( $z$ , lower row) string polarization recorded by the optical sensors as well as the output of the pickup (lower row) are plotted. String velocity waveshapes are normalized to the maximum value of the excitation polarization.

energy, defined as  $E = \int_0^{+\infty} |x(t)|^2 dt$ . It confirms the validity of the wire-breaking method: One polarization gets excited a lot more than the other, so the polarizations can be studied separately. The 20 measurements all exhibit the same pickup behavior: The waveshape of the pickup signal is a lot more similar to the waveshape of the  $z$  string polarization than it is to the  $y$  string polarization. Figure 10 tends to show that the “preferred” string polarization with respect to the pickup behavior is the out-of-plane one.

## 2. Pickup's output signal content in playing conditions

In order to show that the pickup is more sensitive to the  $z$  polarization of the string vibration, the recordings of the G3 string notes of Sec. II B are used. The plucking is typical of a normal playing plucking, that is a combination of  $y$  and  $z$  excitation. The ESPRIT method is expected to identify two components in the output signal of the pickup: a high- and a low-amplitude component corresponding to the  $z$ - and  $y$ -polarization, respectively. Figure 11 shows the identified  $Q$

factors for the both polarizations of the fundamental frequency of every note of the G3 string. The dead spots at 9th fret ( $y$ -polarization) and 12th fret ( $z$ -polarization) are undoubtedly identified, and are the only dead spots along this string, as it can be expected from Fig. 7. In Fig. 11, the circles' radii are proportional to the amplitude of the both polarizations, normalized to the amplitude of the  $z$ -polarization. The series of identified components that takes a low  $Q$ -value at 12th fret consistently has a much larger amplitude than the series that takes a low  $Q$ -value at 9th fret. The high- and low-amplitude components are then confirmed to be associated with out-of-plane and in-plane string polarization, respectively. The pickup of this study is more sensitive to the  $z$ -polarization than to the  $y$ -polarization.

This polarization-dependent sensitivity of the pickup tempers the unwanted nature of dead spots: an abnormal damping for the  $y$ -polarization is likely to disturb the guitarist when he plays the unplugged guitar, but the  $y$ -polarization is almost not transduced by the pickup, so when the guitar is plugged the dead spot is not heard in the amplified sound.

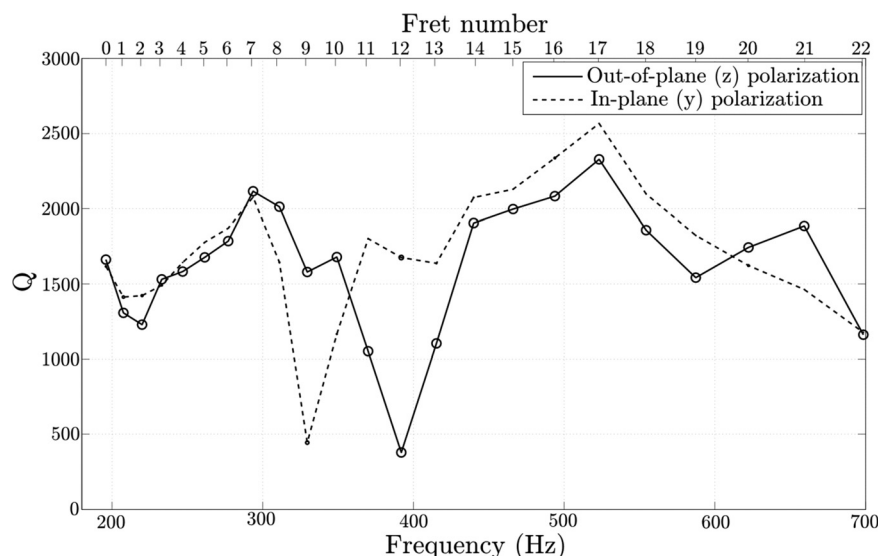


FIG. 11. Identified  $Q$  values associated with the fundamental frequency of both string polarizations. The analyzed signal is the output of the pickup, for each note played on the G3 string mounted on the guitar. Solid line is for the out-of-plane ( $z$ ) polarization and dashed line for the in-plane ( $y$ ) polarization. For each fret, circles' radii indicate the amplitude of the polarizations, normalized to the amplitude of the  $z$ -polarization.



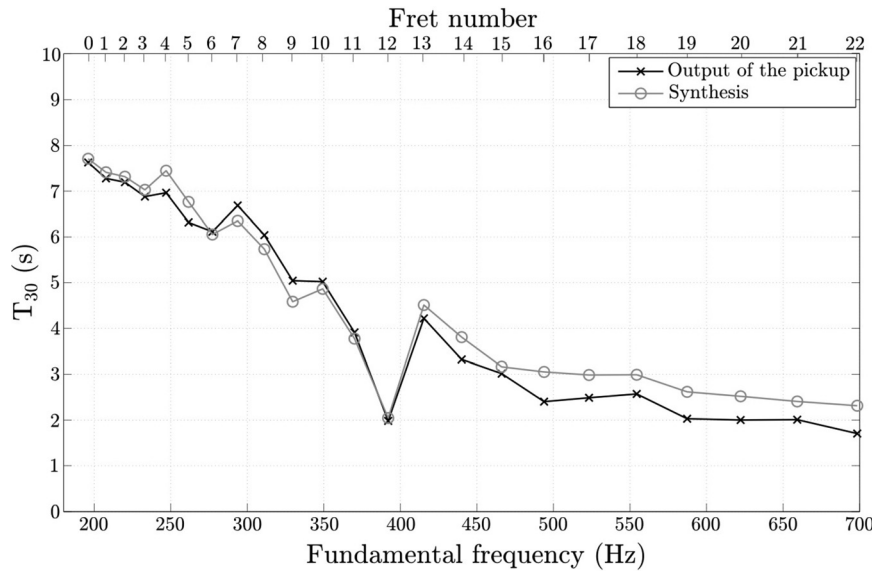


FIG. 12. T30 for each fret of the G3 string. Gray circles indicate T30 values computed from the synthesized signal. Black crosses indicate T30 values computed directly from the output signal of the pickup.

## V. ACCURATE PREDICTION OF THE DECAY TIME

This section proposes a comparison between measured and synthesized decay times. The first is computed from real guitar signal recordings. The second is computed from synthesized signals based on experimental data obtained on the isolated string and on the structure.

On the one hand, the decay time is computed from recordings. Once again, the output of the pickup is recorded. The notes of the third string are plucked with a pick by the experienced player and fingered by a capo for frets 1 to 15 and by the left-hand middle finger for frets 16 to 22. For each note, let  $s_{\text{pick}}(t)$  be the output signal of the pickup, low-pass-filtered with a cutoff frequency at 1000 Hz. The energy decay curve (EDC) is derived with the backward integration method:<sup>41</sup>

$$\text{EDC}(t) = \int_t^T s_{\text{pick}}^2(\tau) d\tau, \quad (21)$$

where  $T$  is the total length of the signal. In practice, the EDC is computed where the exponential sinusoid model is valid, typically from two seconds after the start of the signal to the end of the signal. A linear regression of the EDC is computed, from which the decay time T30 is calculated. This corresponds to the time needed by the EDC to decrease by an amount of 30 dB from its maximum level. This gives the “experimental T30.”

On the other hand, a synthesis is computed starting from Eq. (7). Only the  $z$ -polarization is taken into account in the synthesis. The  $f_n$  are the flexible string frequencies and are in a harmonic relationship with a known fundamental frequency. The upper limit of the bandwidth is 1000 Hz. All components below this limit are taken into account.  $N$  denotes the number of components in the bandwidth. The  $\phi_n$  are randomly generated (T30 results are very similar for  $\phi_n = 0$  for all  $n$ ). The  $a_n$  are set to a theoretical value for a string with a triangle initial displacement and a null initial velocity.<sup>42</sup> Denoting  $h$  the initial plucking height,  $x_p = 4$  cm the plucking point and  $x_m = 12$  cm the measurement point, the synthesized velocity signal is

$$s_{\text{syn}}(t) = A_{\text{vel}} \sum_{n=1}^N \frac{\sin(k_n x_p) \sin(k_n x_m) \sin(2\pi f_n t)}{n} e^{-(\pi f_n / Q_n) t}, \quad (22)$$

where  $A_{\text{vel}} = -2hLc / [\pi x_p (L - x_p)]$  and  $Q_n$  are the results of Eq. (20), a combination of isolated string damping and damping via coupling with the structure. If the measured signal  $s_{\text{pick}}(t)$  and the synthesized signal  $s_{\text{syn}}(t)$  are normalized to their respective maximum value, the term  $A_{\text{vel}}$  in Eq. (22) can be set to 1. A linear regression of Eq. (21) with  $s_{\text{syn}}$  instead of  $s_{\text{pick}}$  gives the “synthesized T30.”

Figure 12 shows the experimental and synthesized T30 for each note of the G3 string. A good agreement is found between the T30 from the pickup’s output signal and the T30 from the synthesis. A slight difference between the two T30 can be seen at some frets. This difference nonetheless never exceeds 0.6 s, which is small in comparison with the more-than-2-s gap observed between the dead spot at fret 12 and its neighbors. Note that for fret 12 the string and structure frequencies do not exactly coincide (see Fig. 8) so the difference in boundary conditions (free conditions for the structure investigation, playing conditions for the note recording) do not affect a lot the T30. In conclusion the trends in the experimental T30 curve shape are well identified by the synthesis: dead spots are found and definitely predicted.

## VI. CONCLUSION AND PERSPECTIVES

In this article a series of assumptions and simplifications that are usually made for the mechanical study of the electric guitar is checked theoretically and experimentally. Considering only the out-of-plane polarization of the string connected to its end on the neck’s side to an out-of-plane mobility is shown to be a good approximation of the mechanical interactions in the electric guitar. This simple model gives quantitative predictions that fit well the measurements. The knowledge of the isolated string  $Q$  factors and the vibrational behavior of the structure is sufficient to accurately estimate the decay time of the final signal, which is the

output of the pickup. Indeed the pickup has been shown to not have a measurable influence on the decay time.

The design of a predictive tool for dead spots and timbral unevenness is then readily possible. Most of the information that predicts the decay time is contained only in the isolated string  $Q$  factors and in the conductance values on the neck. Given an electric guitar string, isolated string  $Q$  factors are only to be measured once. As for the conductance values of the neck, it is a very time-consuming task to carry out all the measurements. Finite-element modeling is an alternative to get this whole conductance data. Provided the geometry of the instrument, the material constants (Young's moduli, density,...) identified on wood samples, and a single mobility measurement giving the modal dampings (conductance peak heights) of the structure, all the conductance values needed can be obtained. The use of a numerical model readjusted with some measurements could be of great help in an industrial context of solid body electric guitar manufacturing.

Results are given here for one string. The coupling of the other strings with the guitar is described in an identical way. A database giving the  $Q$  factors for other strings (diameters, materials, wound, or flat string) would be extremely valuable.

It is experimentally shown that the pickup converts mainly the out-of-plane string polarization. A pickup model giving the transfer function between the 2D-string velocity and the output voltage of the pickup may confirm the experimental data presented here.

This paper investigated the decay part of electric guitar tones. A precious counterpart of this study would be a focus upon the attack part of the tones. In this study, the linear model is valid. However, the electric guitar playing techniques can sometimes lead to non-linear string vibration: the string amplitudes resulting from tough pick strokes can exceed the small values needed for a linear description of the vibration. Other slight non-linear phenomena can also result from end conditions when taking into account the shape of the bridge and frets, or the friction between the string and the fret. This will be the purpose of further studies.

## ACKNOWLEDGMENTS

The authors thank the luthiers Vincent Charrier, Loïc Keranform, Lisa Marchand, Bela Pari, Alexandre Paul, Julien Simon, who built and lent the guitars for the present study, as well as their instructors Yann-David Esmans, Fred Pons, and Pierre Terrien. Thanks also to Vincent Dautaut. Thanks to Benoît Navarret and Rémi Blandin for all the helpful discussions.

- <sup>1</sup>A. Paté, B. Navarret, R. Dumoulin, J.-L. Le Carrou, B. Fabre, and V. Dautaut, "About the electric guitar: A cross-disciplinary context for an acoustical study," in *Proceedings of Acoustics 2012*, Nantes, France, pp. 2717–2722.
- <sup>2</sup>R. M. French, *Engineering the Guitar* (Springer, New York, 2009), pp. 81–82.
- <sup>3</sup>D. Queen, "From boom boxes to Beatles, Baez and Boccherini, the electric guitar at the crossroads," in *Proceedings of the 31st Convention of the AES* (1966), paper 450.
- <sup>4</sup>N. G. Horton and T. R. Moore, "Modeling the magnetic pickup of an electric guitar," *Am. J. Phys.* **77**(2), 144–150 (2009).

- <sup>5</sup>T. Jungmann, "Theoretical and practical studies on the behaviour of electric guitar pick-ups," Master's thesis, Fachhochschule Kempten/Helsinki University of Technology, Helsinki, Finland, 1994.
- <sup>6</sup>G. Lemarquand and V. Lemarquand, "Calculation method of permanent-magnet pickup for electric guitars," *IEEE Trans. Magn.* **43**(9), 3573–3578 (2007).
- <sup>7</sup>I. Cohen and T. Hélie, "Real-time simulation of a guitar power amplifier," in *Proceedings of DAFx10* (2010), paper 45.
- <sup>8</sup>J. Macak and J. Schimmel, "Real-time guitar tube amplifier simulation using an approximation of differential equations," in *Proceedings of DAFx10* (2010), paper 12.
- <sup>9</sup>O. Kröning, K. Dempwolf, and U. Zölzer, "Analysis and simulation of an analog guitar compressor," in *Proceedings of DAFx11* (2011), pp. 205–208.
- <sup>10</sup>M. Holters and U. Zölzer, "Physical modeling of a wah-wah effect pedal as a case study for application of the nodal DK method to circuits with variable parts," in *Proceedings of DAFx11* (2011), pp. 31–36.
- <sup>11</sup>N. Lindroos, H. Pettinen, and V. Välimäki, "Parametric electric guitar synthesis," *Comput. Music J.* **35**(3), 18–37 (2011).
- <sup>12</sup>M. Karjalainen, H. Pettinen, and V. Välimäki, "More acoustic sounding timbre from guitar pickups," in *2nd COST G-6 Workshop on Digital Audio Effects* (1999).
- <sup>13</sup>T. Zwicker and S. Buus, "When bad amplification is good: Distortion as an artistic tool for guitar players," *J. Acoust. Soc. Am.* **103**, 2797 (1998).
- <sup>14</sup>J. J. Fricke, "Jimi Hendrix' use of distortion to extend the performance vocabulary of the electric guitar," *J. Acoust. Soc. Am.* **103**, 2797 (1998).
- <sup>15</sup>G. Evangelista, "Physical model of the string-fret interaction," in *Proceedings of DAFx11* (2011), pp. 345–351.
- <sup>16</sup>G. U. Varieschi and C. M. Gower, "Intonation and compensation of fretted instruments," *Am. J. Phys.* **78**(1), 47–55 (2010).
- <sup>17</sup>J. Lane and T. Kasparis, "A frequency error model for fretted string instruments," *Acta Acust. Acust.* **98**, 936–944 (2012).
- <sup>18</sup>C. E. Gough, "Acoustical studies of stringed instruments using string resonances," in *Proceedings of SMAC83* (1983), pp. 19–45.
- <sup>19</sup>G. Weinreich, "Coupled piano strings," *J. Acoust. Soc. Am.* **62**(6), 1474–1484 (1977).
- <sup>20</sup>J. Woodhouse, "Plucked guitar transients: Comparison of measurements and synthesis," *Acta Acust. Acust.* **90**, 945–965 (2004).
- <sup>21</sup>N. H. Fletcher, "Analysis of the design and performance of harpsichords," *Acustica* **37**, 139–147 (1977).
- <sup>22</sup>J.-L. LeCarrou, J. Frelat, A. Mancel, and B. Navarret, "Guitare électrique: Quel rôle pour les éléments de lutherie?" ("Electric guitar: What role for the lutherie parameters?"), in *10ème Congrès Français d'Acoustique (10th French Congress on Acoustics)* (2010).
- <sup>23</sup>D. Russell, W. S. Haveman, W. Broden, and N. P. Weibull, "Effect of body shape on vibration of electric guitars," *J. Acoust. Soc. Am.* **113**, 2316–2316 (2003).
- <sup>24</sup>E. Esposito, C. Santolini, and L. Scalise, "Axe work II: Vibro-acoustical study of solid body electric guitars," in *5th International Conference on Vibration Measurements by Laser Techniques*, Proc. SPIE 4827, 207–218 (2002).
- <sup>25</sup>E. Esposito, "A comparative study of the vibro-acoustical behaviour of electric guitars produced in different decades," in *Proceedings of the Stockholm Music Acoustics Conference (SMAC 03)* (2003), pp. 125–128.
- <sup>26</sup>H. Fleischer and T. Zwicker, "Mechanical vibrations of electric guitars," *Acta Acust. Acust.* **84**, 758–765 (1998).
- <sup>27</sup>H. Fleischer and T. Zwicker, "Investigating dead spots of electric guitars," *Acta Acust. Acust.* **85**, 128–135 (1999).
- <sup>28</sup>H. Fleischer, "Vibration of an electric bass guitar," *Acta Acust. Acust.* **91**, 247–260 (2005).
- <sup>29</sup>D. Hunter, *The Guitar Pickup Handbook* (Backbeat Books, Hal Leonard, New York, 2008), p. 41.
- <sup>30</sup>D. Chadeaux, J. L. Le Carrou, B. Fabre, and L. Daudet "Experimentally based description of harp plucking," *J. Acoust. Soc. Am.* **131**, 844–855 (2012).
- <sup>31</sup>C. Valette, "The mechanics of vibrating strings," in *Mechanics of Musical Instruments*, edited by A. Hirschberg, J. Kergomard, and G. Weinreich (Springer Verlag, Wien, 1995), pp. 115–183.
- <sup>32</sup>F. Rigaud, B. David, L. Daudet "A parametric model and estimation techniques for the inharmonicity and tuning of the piano," *J. Acoust. Soc. Am.* **133**, 3107–3118 (2013).
- <sup>33</sup>J. Woodhouse, "On the synthesis of guitar plucks," *Acta Acust. Acust.* **90**, 928–944 (2004).

- <sup>34</sup>C. Cuesta, "Corde vibrante isolée mécaniquement, amortissements, non-linéarités; application au clavecin et à la tampoura" ("Mechanically isolated vibrating string, damping, non-linearity; application to the harpsichord and the tamera"), Ph.D. thesis, Université du Maine, Le Mans, France, 1990.
- <sup>35</sup>C. Cuesta and C. Valette, "Time-evolution of the vibration of the strings of a harpsichord," *Acustica* **66**, 37–45 (1988).
- <sup>36</sup>C. Cuesta and C. Valette, "Harpsichord string transient vibration on attack," *Acustica* **66**, 112–122 (1989).
- <sup>37</sup>R. J. Hanson, "Optoelectronic detection of string vibration," *Phys. Teach.* **25**, 165–166 (1987).
- <sup>38</sup>R. Roy, A. Paulraj, and T. Kailath, "Esprit: A subspace rotation approach to estimation of parameters of cisoids in noise," *IEEE Trans. Acoust., Speech, Signal Process.* **34**, 1340–1342 (1986).
- <sup>39</sup>J.-L. LeCarrou, F. Gautier, and R. Badeau, "Sympathetic string modes in the concert harp," *Acta Acust. Acust.* **95**, 744–752 (2009).
- <sup>40</sup>B. Elie, F. Gautier, and B. David, "Macro parameters describing the mechanical behavior of classical guitars," *J. Acoust. Soc. Am.* **132**, 4013–4024 (2012).
- <sup>41</sup>M. R. Schroeder, "New methods of measuring reverberation time," *J. Acoust. Soc. Am.* **37**, 409–412 (1965).
- <sup>42</sup>N. H. Fletcher, "Plucked strings—A review," *Catgut Acoust. Soc. Newsl.* **26**, 13–17 (1976).

Copyright of Journal of the Acoustical Society of America is the property of American Institute of Physics and its content may not be copied or emailed to multiple sites or posted to a listserv without the copyright holder's express written permission. However, users may print, download, or email articles for individual use.